Light Yield Studies of the ATLAS Tile Calorimeter

J.G.Saraiva[1,2], S.Néméćek[3], A.Maio[1,2,4]

(1) LIP-Lisboa, Laboratório de Instrumentação e Física Experimental de Partículas

(2) CFNUL, Centro de Física Nuclear da Universidade de Lisboa

(3) Institute of Physics Acad. of Sciences of the Czech Rep. (ASCR)

(4) Faculdade de Ciências da Universidade de Lisboa

The number of photoelectrons per unit of deposited energy (N_{pe}) was determined for 6 Central Barrel modules of the TileCal/ATLAS detector. Test beam data from 2001 to 2003 of 180 GeV muon beams normal to the tile surface, are used. These results are compared with the light yield and PMT quantum efficiency measured in laboratory with radioactive sources and LED respectively. The influence of the N_{pe}'s on the energy resolution and signal to noise ratio is discussed.

Contents

1. Introduction

The number of photoelectrons is one of the parameters that characterizes the performance of a scintillation detector. It can influence the energy resolution, precision limits and the ability to separate physical signals from electronic noise, namely in the detection of muons with TileCal. In the long term operation of TileCal, control or monitorization of, the number of photoelectrons can be used as an aging diagnostic tool. Using prototypes of the TileCal modules it was verified that above 48 pe/GeV, the number of photoelectrons becomes a sub-dominant effect in the determination of the energy resolution for muons [1].

During the tests of production modules the number of photoelectrons has been measured using high energy muons. Beams of 180 Gev with a perpendicular incidence over the tile plane surface, i.e. 90°, are used. The number of photoelectrons have been obtained using a relation based on a Poisson statistics that describes the electron-emission processes at the photocathode. From this principle and introducing a set of parameters that characterize a detector, such as

C as the Excess Noise Factor - ENF for the photodetectors;

α as the energy scale for electrons with units of pC/GeV;

$\frac{\mathbf{e}}{\mu}$ as the ratio of ionization losses for electrons $\left(\frac{dE}{dx}\right)_e^{ionization}$ and muons $\left(\frac{dE}{dx}\right)_\mu^{ionization}$;

the following expression is deduced giving the N_{pe} in pe/GeV[2]:

$$N_{pe} = \frac{\alpha \times C}{Q_{u+d}} \times \frac{\mu}{e} \times \left(\frac{Q_{u+d}}{\sigma^c_{u-d}}\right)^2 \tag{1}$$

where,

$\mathbf{Q_{u+d}} = \mathbf{Q_u} + \mathbf{Q_d}$ is the charge (pC) sum of the two PMT's contribution in a TileCal cell. The letters u and d are a reference to each of the PMT (Up and Down) that read the same cell;

$\sigma^{\mathbf{c}}_{\mathbf{u-d}} = \sigma(Q_u - Q_d) \ominus \sigma_o(Q_u - Q_d)$ where the σ_o corresponds to PMT's pedestal, where the symbol $\ominus$ represents the difference in quadrature.

Eq. 1 has been used as a common tool for the calculation of the number of photoelectrons [3] [4]. This expression is the base of the Slice Method [5], already used for measurements with prototypes of the TileCal modules [6]. In the current document the Slice Method is applied for the calculation of the N_{pe}. The event energy reconstruction in the used data sets was made with the Flat Filter method.

As already mentioned it is necessary to introduce scaling factors and this will be used not considering any errors. However such uncertainties should not be ignored and a brief overview is now presented:

- The measured average of the electrons energy scale factor α has been established to be $\sim 1.2\ pC/GeV$ (Flat Filter). Between modules differences of $\pm 5\%$ are observed. In this note $\alpha = 1.2\ pC/GeV$ will be used independent of the module and no errors will be considered;

- In this note $\frac{e}{\mu} = 0.91$ [7] will be used independently of the module and no errors will be considered;

- The ENF from the measurements reported within the collaboration [8] has values from 1.23 to 1.35, i.e., a difference of 10% between maximum and minimum. For scaling reasons a fixed value of 1.25 is used in order to obtain the correct level of photostatistics and for comparison with earlier calculations.

2. Photostatistics analysis methodology

Muon beams of 180 GeV are used in the present analysis. With such energy a muon can cross all the length of a TileCal module and enable us to study the detector in a cell to cell basis. This analysis uses muon beams perpendicular to the tile surface plan — ATLAS $R\Phi$ plan. For each module and for each tilerow, data are taken for two incidences: $\theta = +90^\circ$ and $\theta = -90^\circ$ — where the '**+**' and '**-**' represent the module η side facing the beam. The resulting numbers can the be compared with the number of photoelectrons resulting from the LASER pulse monitoring system [9].

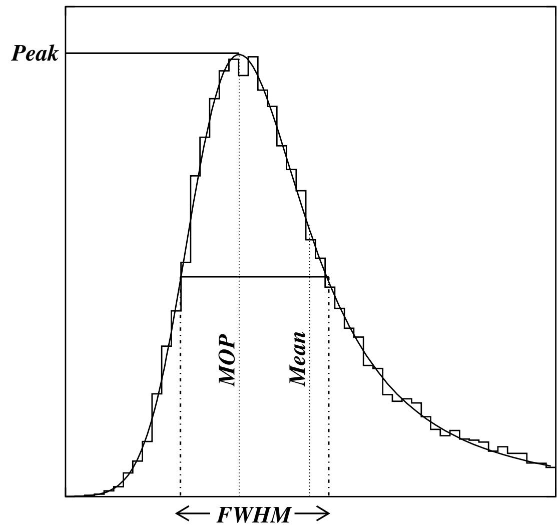

Figure 1: A typical histogram of the deposited energy for a muon beam in the TileCal. The most probable value (MOP) is pointed out as well as the mean (MEAN) value. Due to the longer tail on the high energy side of the peak the $MEAN > MOP$

2.1. Energy distribution from muons in TileCal

In Figure 1 the muon response in a TileCal cell for 180 GeV muons at 90° is depicted. The most relevant quantities characterizing the response are indicated in the figure. A parameterization of a Landau distribution convoluted with a Gaussian distribution is the best description of the energy deposited by muons on a TileCal cell. In the figure it is the continuous smooth line drawn over the histogram. The used function to fit the muon spectra is described in [10].

2.2. Slice Method

To extract the light yield information from the muon response the first step is to get the most probable value (MOP) and full width at half maximum (FWHM) of the muon response using the expression mentioned above. Using the calculated MOP and FWHM a region of interest is defined cutting out the distributions tails. This region of interest should contain the FWHM and is divided in slices of equal size — five in the present analysis (Figure 2(a)). The rms - $\sigma_i^2(u-d)$ - and average

Year	Month	Module
2001	August	JINR 18
2002	June	JINR 34
	July	JINR 55
	August	JINR 01
2003	June	JINR12
	July	JINR 27
	August	JINR 63
	August	JINR 13

Table 1: Central Barrel modules studied in the beam tests at CERN/SPS from 2001 to 2003.

energy - $Q_i(u+d)$ - for all events with energy within each slice i are used. Replacing Q by Q_i we can re-write Eq. 1 as,

$$\sigma_i^2(u-d) = \frac{\alpha \times C}{Q_i(u+d)} \times \frac{\mu}{e} \times \frac{Q_i^2(u+d)}{N_{pe}} + \sigma_o^2(u-d) \tag{2}$$

where $i = 1, \ldots, n$ is the slice index. A linear relation is established between the $\sigma_i^2(u-d)$ and the $Q_i(u+d)$ as shown in Figure 2(b). The N_{pe} is taken from the slope of the fit of experimental data as implied by Eq. 2. The constant term $\sigma_o(u-d)$ is the rms of the pedestal, that in the present analysis is set to the PMT's pedestal measurements, i.e., used as a fixed parameter in the fit.

3. Results and Discussion

This analysis refers to data taken from 2002 to 2003 TileCal test beam periods (TB) at the CERN/SPS; data from 2001 was not used. In Table 1 the tested modules are listed by month and year. In Appendix B a commentary is given on the presented values related to a setting of PAW, that selects between the use of binned or unbinned mean and rms, but this does not bring any significant changes to the present discussion; however for a question of precision the awareness is raised.

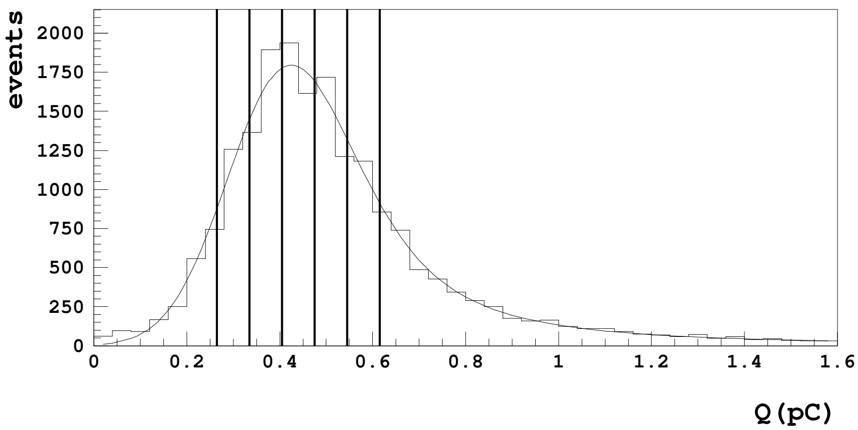

(a) The energy window determined by the MOP and the FWHM is shown. The window is defined in order to contain the full width of the curve at the half maximum.

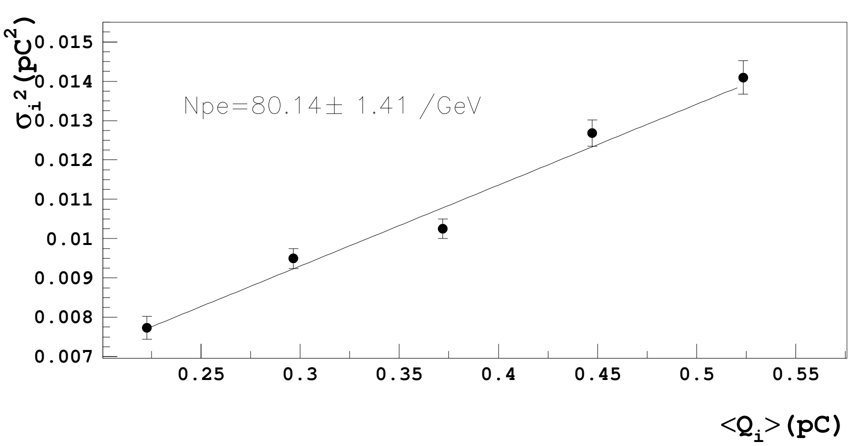

(b) σ^2_{u-d} vs $Q_i(u+d)$ – The slope coming out of the linear fit gives the N_{pe} (Cell A2)

Figure 2: The Slice Method

JINR	−90°			+90°		
27	# cells	N_{pe}	rms%	# cells	N_{pe}	rms%
A	56	78.1	14.6	54	68.0	13.3
B	46	80.9	12.3	45	79.6	11.3
C	43	81.7	11.6	38	78.3	11.6
D	14	99.6	7.6	14	97.5	5.3

Table 2: Example of summary table as in Appendix A. The number of cells used and the average and rms as percentage for the the 4 cell types. The N_{pe} is the number of photoelectrons per GeV

3.1. General remarks

The N_{pe} was measured for each cell of a module (45 cells in a barrel module). The complete set of results, in order to facilitate the reading, are presented in Appendix A.1 for 2002 TB and in Appendix A.2 for 2003 TB. Table 2 presents a summary. The numbers are organized per module and angle of incidence. For each module the results are summarized by the average and rms for each cell type: A,B,C and D. The rms [1] is given as percentage. For each case the number of cells used for the calculation of each number is also given. Although for the barrel calorimeter the B and C cells are grouped in BC cells, i.e. are readout by a unique pair of PMT's, for the following discussion they are considered in separate.

Looking at all the results it can be observed that A cells show the smallest N_{pe} values and the D cells the highest. For some modules D cells are very close to B and C cells, $N_{pe}^{A} < N_{pe}^{B} \simeq N_{pe}^{C} \lesssim N_{pe}^{D}$. One exception is for JINR 01 where the cells A and D show comparable values (77 and 74 pe/GeV respectively) but smaller than the ones in B and C cells (81 and 82 pe/GeV respectively). For all modules the B

[1] The average and rms of a set of calculated values of N_{pe} with dimension equal to (number of tilerows) × (number of cells). For the central barrel modules:

$$\begin{aligned} Acells &\rightarrow 3Tilerows \times 20Cells \\ Bcells &\rightarrow 3Tilerows \times 18Cells \\ Ccells &\rightarrow 3Tilerows \times 16Cells \\ Dcells &\rightarrow 2Tilerows \times 7Cells \end{aligned}$$

Cell	2002 (JINR 01)				2003 (JINR 13)			
	$-90°$		$90°$		$-90°$		$90°$	
	N_{pe}	rms%	N_{pe}	rms%	N_{pe}	rms%	N_{pe}	rms%
A	77.0	7.7	73.2	8.0	72.5	13.3	63.1	14.3
B	81.3	6.7	81.0	8.1	79.5	13.7	80.1	17.3
C	82.5	8.6	82.1	6.4	79.7	11.6	76.5	14.1
D	74.2	6.3	73.3	6.5	84.7	8.6	81.7	6.9

Table 3: The number of photoelectrons per GeV N_{pe} from the SLC method using μ at $-90°$ and $+90°$ for Central Barrel modules JINR 01 and JINR 13

and C cells values are equal within the calculated errors as required. However this is not a trivial result since the B and C cells have tiles from two producers with different light yields [11]. An optical mask was introduced in order to achieve the light yield uniformity for these channels (further details in Section 3.3.1).

In Table 3 data from 2002 (JINR 01) and 2003 (JINR 13) testbeam, for $\theta = -90°$ and for $\theta = +90°$, are presented. When comparing the results for the two years some differences are observed. In the 2002 TB the differences in N_{pe} for data coming from $\theta = -90°$ and from $\theta = +90°$ are of ~ 4 pe/GeV ($\sim 5\%$) are found for A cells but for B and C cells the differences tend to be close to ~ 1 pe/GeV ($\sim 1\%$); the rms varies between 6.3% and 8.6%. For the 2003 TB, and making the same comparison, a large difference of ~ 10 pe/GeV (12.5%) is found in the calculated N_{pe} for the A cells. For the B and C cells the two beam geometries present similar values of N_{pe} but the rms is $\sim 3\%$ higher at $\theta = +90°$ than at $\theta = -90°$, and twice higher than in 2002. The D cells show for the two years a similar performance. These observations are valid for any other pair of modules from the two years.

Any differences between 2002 and 2003 testbeam, related with precision on the positioning and energy of the beam, should not be of significant. However, these results show that during the 2003 testbeam the N_{pe} is extremely dependent on the orientation of the impinging beam. This effect decreases as the cell size increases ($A \rightarrow D$).

3.2. Readout asymmetries

To understand the differences observed in N_{pe} obtained from muons coming from $-90°$ or $+90°$ a more detailed analysis is necessary. A study made on a 'per-cell' basis is presented next. In subsection 3.2.1 the N_{pe} is compared for the two beam geometries, and the readout asymmetries inside a cell are discussed in subsection 3.2.2.

3.2.1. N_{pe} difference between $\theta = -90°$ and $\theta = +90°$

In Figure 3 distributions comparing the N_{pe} for the two beam geometries are presented. The results for each test beam year are combined and the difference

$$D_{N_{pe}} = N_{pe}^{-90°} - N_{pe}^{+90°}$$

and ratio

$$R_{N_{pe}} = \frac{N_{pe}^{-90°}}{N_{pe}^{+90°}}$$

are plotted. These quantities measure the reproducibility of the N_{pe} measurement using the TileCal test beam setup for the two beam geometries. In Table 4 the same quantities are summarized per module using the mean and rms of the distributions alike to those presented in Figure 3.

The discussion will be divided in two parts: first the *mean* values are compared and afterwords a comparison is made over the statistical error

$$\Delta N = \frac{rms}{\sqrt{\#entries}} \qquad .$$

It is seen that modules JINR 55 and JINR 01 (2002 TB) present good reproducibility for the two μ beam geometries as expressed either by the mean values of $D_{N_{pe}}$ or $R_{N_{pe}}$. For JINR 34 and (2002 TB) the reproducibility is poorer and is similar to 2003 TB results. When comparing the ΔN for the two years it is seen that the

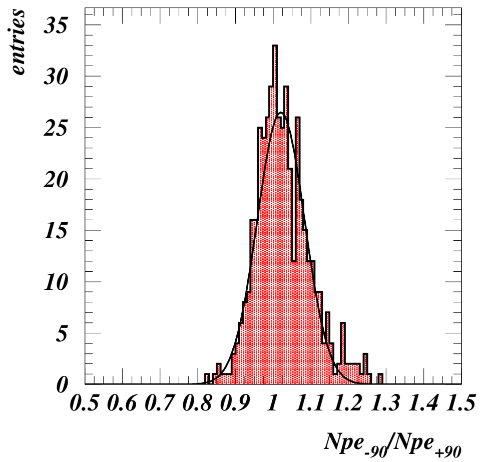

(a) $N_{pe}^{-90^\circ}/N_{pe}^{+90^\circ}$ in 2002 TB

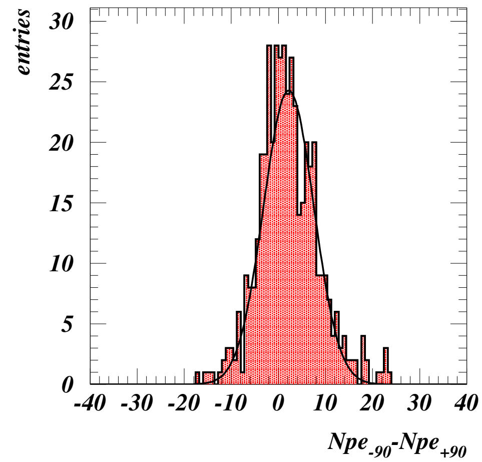

(b) $N_{pe}^{-90^\circ} - N_{pe}^{+90^\circ}$ in 2002 TB

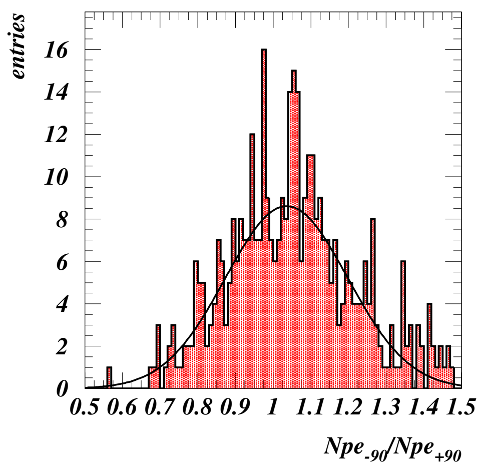

(c) $N_{pe}^{-90^\circ}/N_{pe}^{+90^\circ}$ in 2003 TB

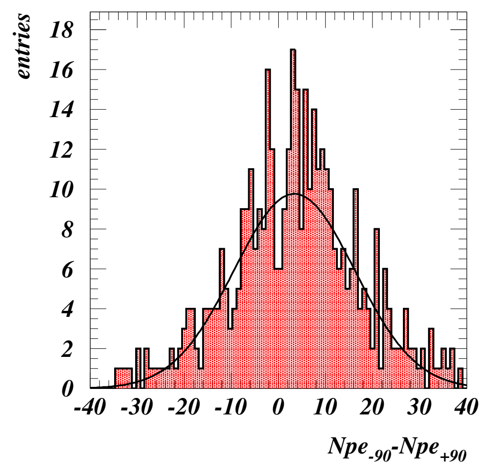

(d) $N_{pe}^{-90^\circ} - N_{pe}^{+90^\circ}$ in 2003 TB

Figure 3: The N_{pe} for -90° and $+90^\circ$ in 2002 TB and 2003 TB. For each year the results from the different modules are combined in a unique histogram. The difference $N_{pe}^{-90^\circ} - N_{pe}^{+90^\circ}$ and the ratio $N_{pe}^{-90^\circ}/N_{pe}^{+90^\circ}$ are presented.

Year	Module	#entries	$N_{pe}^{-90^\circ} - N_{pe}^{+90^\circ}$	$N_{pe}^{-90^\circ}/N_{pe}^{+90^\circ}$
2002	JINR 34	149	4.77 ± 0.67	$1.05 \pm 0.73 \times 10^{-2}$
	JINR 55	158	0.44 ± 0.36	$1.01 \pm 0.47 \times 10^{-2}$
	JINR 01	152	1.53 ± 0.39	$1.02 \pm 0.56 \times 10^{-2}$
2003	JINR 27	155	3.20 ± 0.86	$1.07 \pm 1.44 \times 10^{-2}$
	JINR 63	118	2.45 ± 1.20	$1.05 \pm 1.84 \times 10^{-2}$
	JINR 13	151	3.10 ± 1.05	$1.09 \pm 1.79 \times 10^{-2}$

Table 4: The mean and statistical error (ΔN) for $D_{N_{pe}}$ and $R_{N_{pe}}$

values are consistently higher for the 2003 TB. For the 2002 TB the worse value of rms is for the module JINR 34 which also has the larger difference in the mean value of the two quantities in discussion. Before drawing out some conclusions a look over the cells readout asymmetries is presented, comparing the charge signal of the pair of PMT's of a cell.

3.2.2. UP/DOWN charge asymmetry

The difference observed in the measurement of N_{pe} for $\theta = -90°$ and $\theta = +90°$ during 2002 and 2003 can be related with the difference between the signal measured by the two photomulipliers in a TileCal cell. This difference within a cell is usualy refered as the cell asymmetry and its calculated using

$$A_{ud} = \frac{u - d}{u + d} = \frac{Q_u - Q_d}{Q_u + Q_d}$$

for each cell of a module. The A_{ud}'s in the two TB years using the $\theta = \pm 90°$ scans are compared.

In Table 5 the A_{ud} is summarized for the two barrel modules JINR 01 from 2002 and JINR 13 from 2003 testbeam. For each cell type the mean value and corresponding rms of this quantity are presented. The 2002 TB module JINR 01 has a mean value that varies between 1.57% and 2.83% meaning this that the beam is shifted from the cell center but the difference between samplings for A_{ud} is not

Cell	JINR 01		JINR 13	
	$\theta = -90°$	$\theta = +90°$	$\theta = -90°$	$\theta = +90°$
A	1.58±1.77	2.76±1.99	2.36 ±3.61	6.30 ±8.07
B	2.07±1.54	2.83±1.61	1.17 ±3.43	3.69 ±6.44
C	2.09±1.51	2.43±1.73	0.28 ±3.28	1.20 ±4.68
D	1.40±1.55	1.57±2.19	-0.45±2.51	-0.53±2.71

Table 5: Readout asymmetries (A_{ud}(%)) for the CB modules JINR 01 (2002 TB) and JINR 13 (2003 TB)

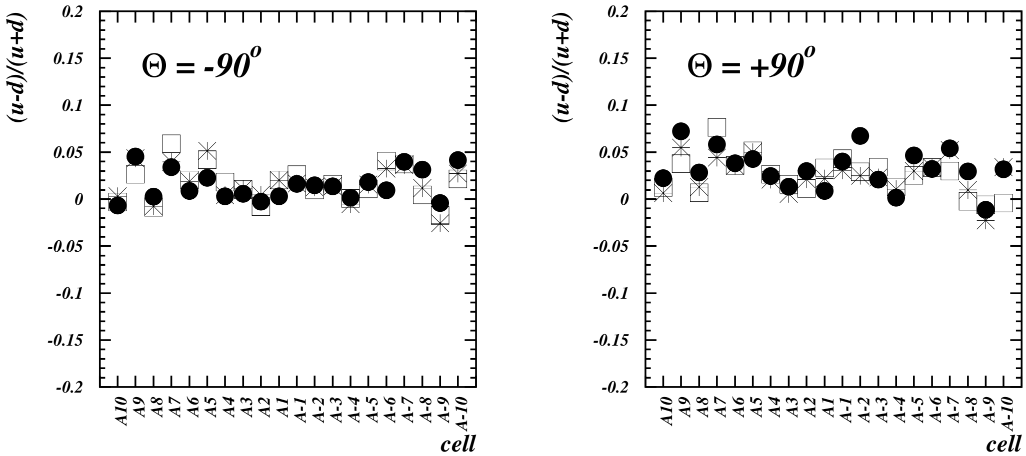

(a) A_{ud} for JINR 01 in 2002 testbeam.

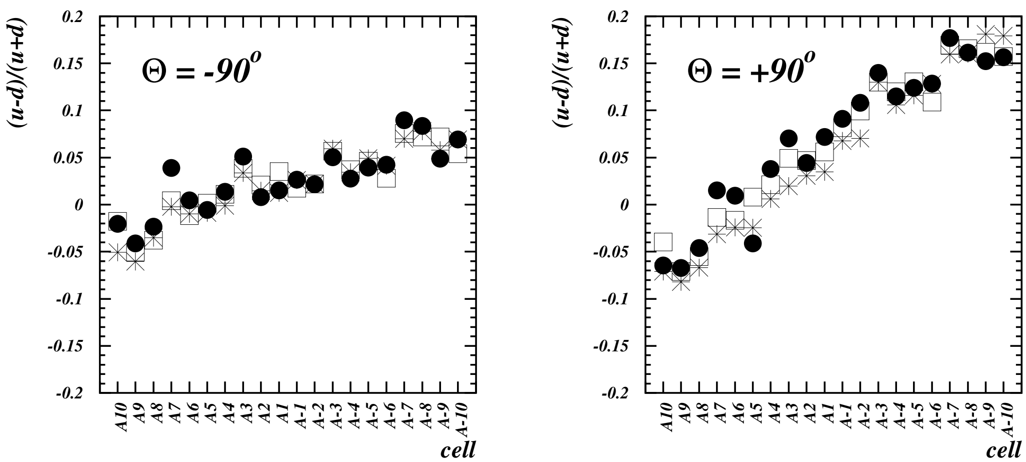

(b) A_{ud} for JINR 13 in 2003 testbeam.

Figure 4: The A_{ud} ratios Vs. Cell number for A cells from CB modules JINR 01 (2002 TB) and JINR 13 (2003 TB). Where the $*$ is for Tilerow 1 ● for Tilerow 2 and ■ for Tilerow 3.

larger than 1.5%. The corresponding rms is always below 3% and independent on the inpinging 'beam direction' [2]. This is not observed for the 2003 TB and in particular for module JINR 13. The mean value of A_{ud} now varies between -0.45% and 6.30% and the rms is almost always above 3%, being the exceptions the D cells. A_{ud} is sensitive to the 'beam direction' with a larger asymmetries for $\theta = +90°$. A_{ud} also has a decreasing tendency as the cell size increases ($A \rightarrow D$).

To illustrate all these comments the results for the A cells are plotted in Figure 4(a) for JINR 01 (2002 TB) and in Figure 4(b) for JINR 13 (2003 TB) for each tilerow scan and for each cell. An hypothesis for these slopes and this dependence with the 'beam direction' is related with the table supporting the modules. During the 2003 TB it was observed that the table could tilt ($\sim 1°$). The resulting effect of this tilt in the muon data are the read-out asymmetries of the type described above that increase (or decrease) along the tilerow (Figure 4(a) and 4(b)).

* * *

Can these differences in A_{ud} produce a measurable effect in the number of photoelectrons? Some correlation is observed between $D_{N_{pe}}$ or $R_{N_{pe}}$ and A_{ud} which could mean that the N_{pe} measurement is sensitive to the beam position and orientation. The main objective of the present analysis is to obtain the value(s) of light yield that can be representative of the TileCal detector. To achieve this, the results from as many modules as possible should be combined but at the same time awareness should be taken to any instrumental effects, or any other kind, that could jeopardize the quality of the final results. In order to include the maximum number of modules and at the same time minimize the effect of the measured asymmetries only runs for $\theta = -90°$ will be used in the next sections.

[2]This is only used to illustrate the problem: the beam is static and is the orientation is given by the position of the table supporting the modules.

Module	Tile Size			
	A 1-3	B 4-6	C 7-9	D 10-11
JINR 01	PSM #1	PSM #1	PSM #1	PSM #1
JINR 12	PSM #1	PSM #1	PSM #1	PSM #1
JINR 13	PSM #1	PSM #1	PSM #1	PSM #1
JINR 18	PSM #2	PSM #3	BASF #3(M)	BASF #3
JINR 27	PSM #2	PSM #3	BASF #3(M)	BASF #3
JINR 34	PSM #2	BASF #4A	BASF #4A	BASF #4A
JINR 55	PSM #2	BASF #4B	BASF #4B	BASF #4B
JINR 63	PSM #2	BASF #4B	BASF #4B	BASF #4B

Table 6: The batches of tiles used in the production Barrel modules under study. M is for Masked, i.e., BASF tiles that were masked to equalize with the light yield of PSM tiles. The number after the tile type refers to the production batch of those particular tiles.

3.3. Tile producer and N_{pe}

In Table 6 the tile distribution for the studied modules is presented, using the information from the online logbook [11]. To identify the tiles a label with a combination of the producer name, PSM or BASF, and a number related with the used batch. A letter M is the indication that the used tiles were masked for a light yield correction. As an example, PSM tiles coming from batch 3 are identified as PSM #3.

3.3.1. Masking

To improve uniformity within cells where BASF and PSM tiles are mixed, the BASF tiles read-out edges were masked. This procedure is illustrated in Figure 5 where an upper section and a bottom section of the readout edge are painted in white. It was necessary to use this extra masking in modules JINR 18 and JINR 27. For these modules, A and B cells are PSM and C and D cells are BASF but the tiles included in the C cells are masked. If the obtained N_{pe} are compared (see Table 2

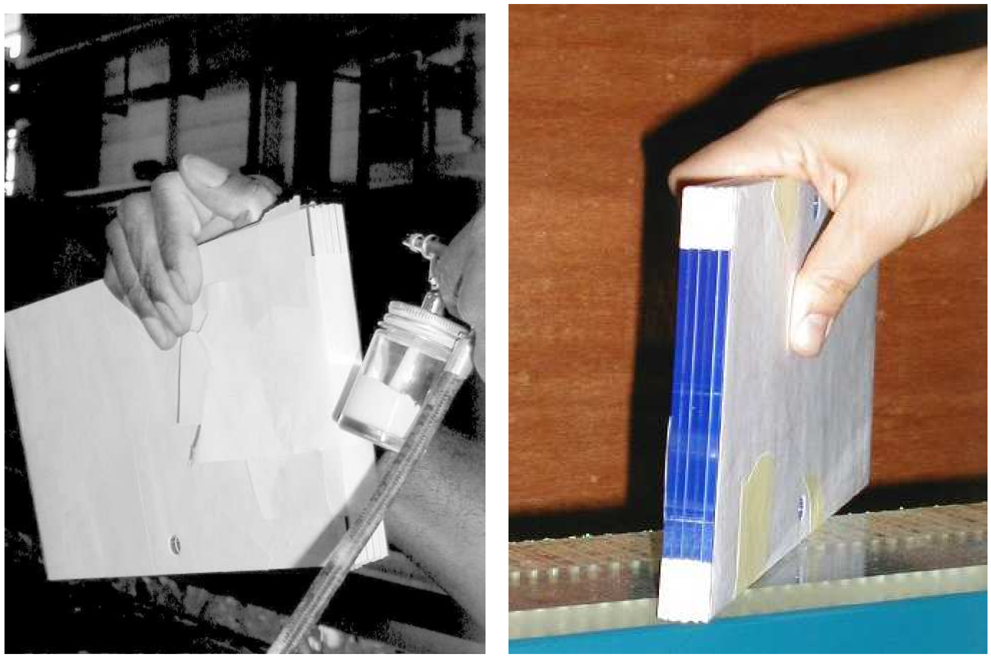

(a) Painting the tiles edges **(b)** The resulting masked tiles

Figure 5: The tile edge masking used to reduce the light yield from the tiles produced by BASF. Upper and lower white bands cover a portion of the readout edge of BASF tiles as a compensation to the larger light yield.

or Table 12 for JINR 27 results) it is verified that B and C cells match very well,

$$N_{pe}^{PSM}(B) \equiv N_{pe}^{MaskedBASF}(C) < N_{pe}^{BASF}(D)$$

and the D cells have an higher N_{pe} .

3.3.2. Comparison with the estimated value of 75 pe/GeV

The number of photoelectrons can be estimated using the energy scale $\alpha = 1.2\,pC/GeV$ defined for electrons impinging at $\theta = 90^\circ$ modules of the calorimeter[3] and the gain defined to be in use in TileCal PMT's, $G = 10^5$. Since the charge at

[3]Recall that this is for the energy reconstructed with the Flat Filter method.

the PMT anode can be expressed as,

$$Q = q_e \times N_{pe} \times G$$

the number of photoelectrons per GeV can be estimated as

$$N_{pe} = \frac{\alpha}{q_e \times G} = 75\ pe/GeV \qquad (3)$$

This is the number obtained for the electrons energy scale. For muons the number should be multiplied by the $\mu/e \simeq 1.09$ factor resulting a value of 82 pe/GeV.

3.3.3. Comparing tile production batches

The results summarized in Table 11 and Table 12 are rearranged by producer and also by production batch in Table 7. Once more the used data comes only from beams at $-90°$.

Table 7 has the N_{pe} values obtained for the central barrel module. The last two columns are the average and rms per batch and the average and rms per tile producer — PSM and BASF — respectively. The used rms is calculated using only the N_{pe} entries in this table, neglecting the rms calculated for each cell type (as presented in Table 11 and Table 12). It is verified that tiles from PSM production and BASF production show a difference of ~ 20 pe/GeV. Typical values of ~ 80 pe/GeV for PSM tiles and ~ 100 pe/GeV for BASF tiles are found. In Figure 6 the plotted values are the averages coming from Table 7. Concluding, the results are insensitive to the batch but a clear difference is observed between producers as mentioned before. For this reason the results are combined maintaining the distinction of tile producer and cell type in Table 6. A scaling factor comparing the light yield of tiles coming from BASF and tiles coming from PSM of

$$BASF/PSM \simeq 1.25$$

PS Type	Batch #	JINR	$N_{pe}(n_{pe}/GeV)$ [$N^{\circ}measurements$]					
			A	B	C	D	N_{pe}^{BATCH}	$N_{pe}^{Polystyrene}$
PSM	1	01	77.0 (54)	81.3 (46)	82.5 (45)	74.2 (12)		
		13	72.5 (53)	79.5 (50)	79.7 (42)	84.7 (14)	78.9±4.1	
	2	34	83.6 (51)	–	–	–		
		55	82.2 (48)	–	–	–	81.0±2.4	79.8± 3.4
		27	78.1 (56)	–	–	–		
		63	79.9 (51)	–	–	–		
	3	27	–	80.9 (46)	81.7 (43)	–	81.3±0.6	
BASF	3	27	–	–	–	99.6 (14)	99.6**	
	4A	34	–	101.9 (45)	100.7 (42)	104.5 (14)	102.7±1.6	100.6± 2.1
	4B	55	–	100.6 (48)	100.3 (48)	98.9 (14)		
		63	–	84.8* (38)	88.7* (35)	97.0 (10)	99.3±1.5	

Table 7: The N_{pe} in each module per cell type and for each scintillating tile producer batch. The used numbers come from the SLC method for −90°. For each module and each sampling the averaged N_{pe} is given with the corresponding number of used cells: N_{pe} (#cells). The errors used in the last two collumns are the absolute rms of the numbers in this table.
(*) Smaller number due to instrumental tests during optics assembly.
(**) Only one data point for batch 3 of BASF and so no rms.

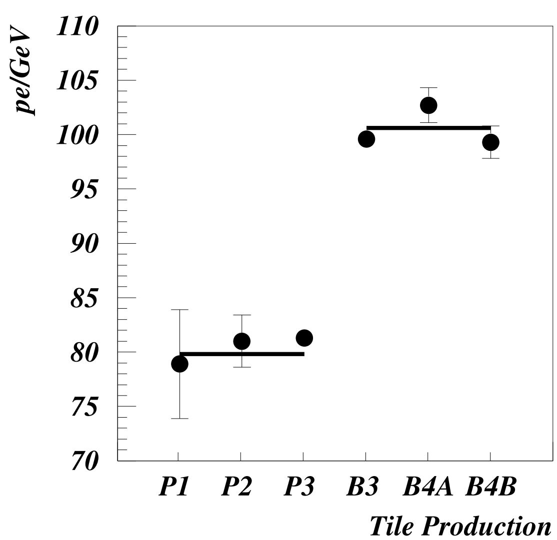

Figure 6: N_{pe} for 3 batches of PSM (P) and BASF (B) tiles. The values are the averages and RMS from results presented in Table 7

Cell type	PSM	BASF
A	78.8 ± 0.5	—
B	80.5 ± 0.8	96.4 ± 1.0
C	81.3 ± 0.9	97.2 ± 0.9
D	79.8 ± 1.6	100.3 ± 1.2

Table 8: The number of photoelectrons per GeV for 90° muons, in Tilecal barrel modules. The average value for each cell type and the respective statistical errors (rms/ $\sqrt{\#cells}$) are given separately for PSM and BASF scintillators.

is obtained in TileCal for the central barrel modules.

3.3.4. N_{pe} vs. Tiles QC

A quantitative comparison can be done between the scintillating tiles light yield data obtained during the quality control (QC) [11] and the N_{pe} results from beam tests. In these measurements the scintillating tile is excited near a readout edge (I_0) where an optical fiber is coupled and in the opposite readout edge (I_1). For the quality control two quantities are used: I_o sensitive to the light yield and I_o/I_1 sensitive to the attenuation length (i.e., light transmission). They are plotted against N_{pe} in Figure 7. A correlation is clear between the I_o and the N_{pe} (Figure 7(a)) as expected, but a clear distinction and correlation is only found between tile producers. Within each producer the fluctuations blur any possible correlation that could be found between batches of the same producer. It is confirmed that the higher light yields as measured during the tiles QC corresponds to the highest number of photoelectrons. For I_o/I_1 no correlation is found with N_{pe} meaning that the attenuation length is the same for the two producers except for the high tail of the I_o/I_1 distribution. It is worth noticing that for the PSM tiles the dispersion of I_o/I_1 is higher with a minimum/maximum ratio of the order of 20%; for BASF tiles this same difference is reduced about 10%.

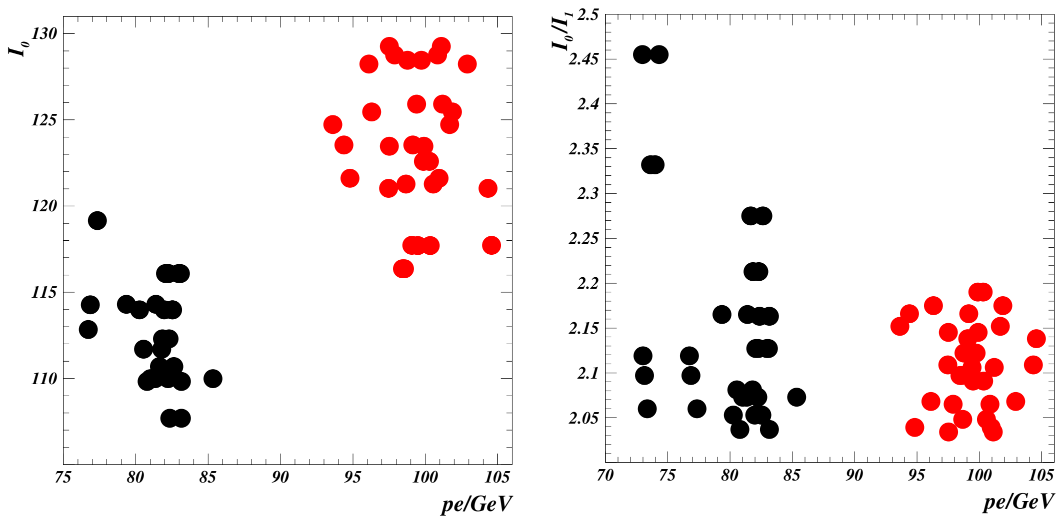

(a) I_o vs. N_{pe} **(b)** I_o/I_1 vs. N_{pe}

Figure 7: The number of photoelectrons N_{pe} as function of I_o/I_1 and I_o the two scintillating tiles QC parameters.

3.4. Quantum efficiency

The N_{pe} is proportional do the ε_q by definition and the ε fluctuations can have a contribution on the measured light yield. The light yield as calculated in the previous sections is plotted against the photomultiplier quantum efficiencies ε_q as in Figure 8 for JINR 34 detailed by the cell type (A, B, C and D). For this module the A cells have tiles made of PSM polystyrene and B, C and D cells have tiles made of BASF polystyrene. The quantum efficiency for each PMT was measured during the PMT acceptance QC. Since the N_{pe} is calculated per cell for each cell the average of the ε_q of the two read-out PMTs is used; which is reasonable since differences between PMT's ε_q are of the order of 1% within a cell. From these plots a clear correlation is not found between the two quantities but this could be hidden by the very large fluctuations, of the order of 10%, in the calculated number of photoelectrons when compared with the quantum efficiency fluctuations of the order of 3%. Even for very small fluctuations on the ε_q as of the order of 0.5%, fluctuations on N_{pe} of the order of 10% are observed.

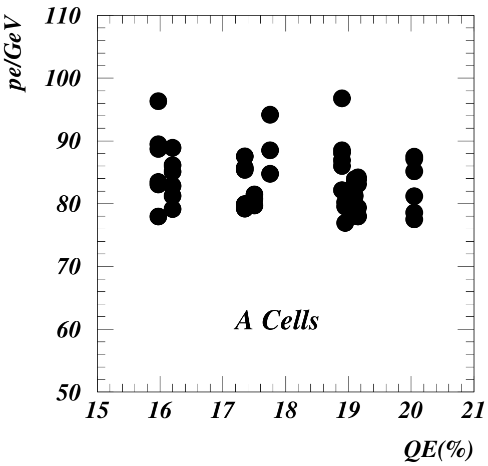

(a) A cells

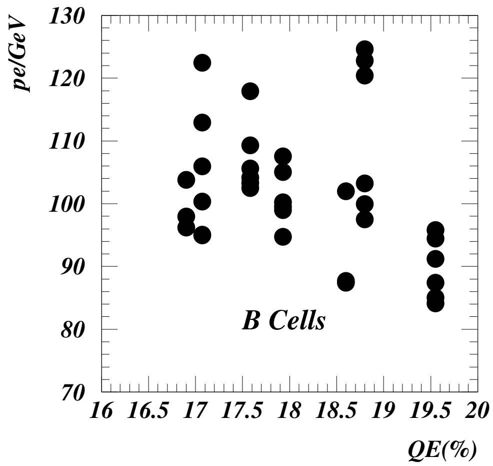

(b) B cells

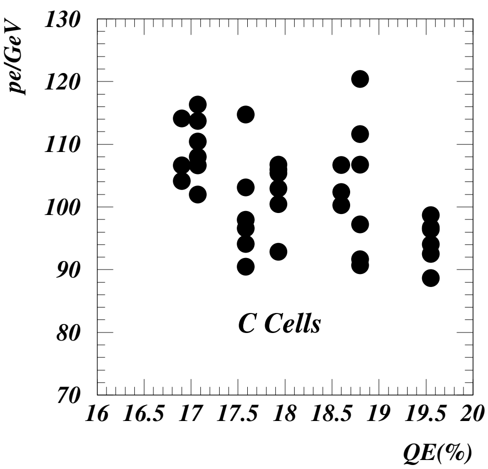

(c) C cells

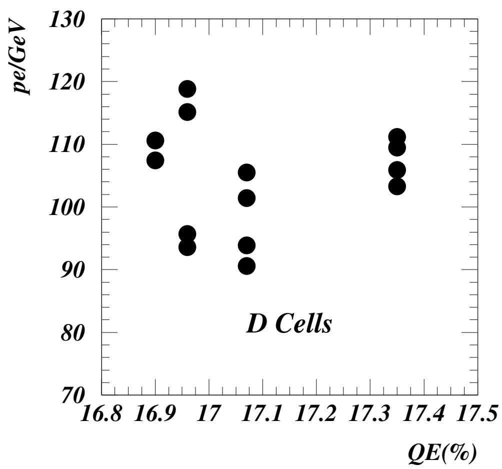

(d) D cells

Figure 8: The N_{pe} for JINR 34 module vs. the PMT quantum efficiency $\varepsilon_q(\%)$. N_{pe} using the SLC method with μ at $-90°$

3.5. N_{pe} and Energy resolution

As was expressed during the motivations to this work the N_{pe} directly contributes to the energy resolution of TileCal. This can be evident when writing a term including only the contribution of photostatistics:

$$\left(\frac{\sigma}{E}\right)_{photostatistics} = \frac{\sigma_{pe}}{n_{pe}} = \frac{\sqrt{n_{pe}}}{n_{pe}} = \frac{1}{\sqrt{n_{pe}}} = \frac{1}{\sqrt{N_{pe} \cdot E}} = \frac{1/\sqrt{N_{pe}}}{\sqrt{E}}$$

where n_{pe} is the absolute number of photoelectrons and σ_{pe} the corresponding distribution width. The energy resolution parameterization has three terms, being the first $\frac{a}{\sqrt{E}}$ the contribution from statistical effects which includes the photostatistics. The parameterization can be naturally extended by presenting the first term as explicitly resulting from two contributions: physics processes (a_1) and photostatistics (a_2):

$$\frac{\sigma}{E} = \frac{a}{\sqrt{E}} \oplus \frac{b}{E} \oplus c = \frac{a_1}{\sqrt{E}} \oplus \frac{a_2}{\sqrt{E}} \oplus \frac{b}{E} \oplus c \tag{4}$$

with $a_2 = 1/\sqrt{N_{pe}}$ and E in GeV.

The N_{pe} measurements presented in the above sections were shown to depended on the tiles polystyrene. In Table 9 the influence of the measured light yield is investigated comparing the measured energy resolution ($a_{exp} = 55\%$) with the one that should be achieved if only $N_{pe} \simeq 20 pe/GeV$ (TDR minimum). Combining the measured N_{pe} and a_{exp} it is obtained the value of the term $< a_1 >$; the a_{calc} is the quadratic sum of $< a_1 >$ and a_2 with $N_{pe} = 20\ pe/GeV$. It is shown that the the energy resolution would be degraded by 3.4% ($a_{calc} - a_{exp}$). The weight of the light yield contribution on the energy resolution can also be obtained for both cases. This is achieved using

$$c_{weight} = \left(\frac{a_{stat} \ominus a_1}{a_{stat}}\right)^2$$

For the N_{pe} measured for the TileCal production modules this weight is of 4%;

<table>
<tr><th>Source</th><th>N_{pe} (pe/GeV)</th><th>$a_2 = 1/\sqrt{N_{pe}}$ (%)</th><th>a_{exp} (%)</th><th>$< a_1 >$ (%)</th><th>a_{calc} (%)</th></tr>
<tr><td>TDR Minimum</td><td>20.0</td><td>22.4</td><td>—</td><td rowspan="3">53.9</td><td>58.4</td></tr>
<tr><td>PSM</td><td>79.8</td><td>11.2</td><td rowspan="2">55</td><td rowspan="2">—</td></tr>
<tr><td>BASF</td><td>100.6</td><td>9.9</td></tr>
</table>

Table 9: Npe influence on Energy Resolution. Comparing present results of energy resolution and light yield to obtain $< a_1 >$; this is an average of the BASF(a_1 = 54.1) and PSM (a_1 = 53.8) calculated values. The a for a 20 pe/GeV light yield (TDR reference value) is calculated for comparison

for 20 pe/GeV it would grow up to 14%. The light yield level of the TileCal detector is well above the TDR minimum of 20 pe/GeV and its impact on the energy resolution it was shown by simple algebra to be around 4%.

3.6. Signal to noise ratio

Since TileCal can be used as a muon trigger in ATLAS a clear distinction between the muon events and the electronic noise events is required. Measurements using prototypes have shown that the width of the muons response was sensitive to the variation of the N_{pe}. For a variation of the N_{pe} from 20 pe/GeV to 48 pe/GeV a variation is observed in the width of the charge distribution. Above 48 pe/GeV no visible change is observed [1]. The S/N is calculated for $\theta = 90^\circ$ and $\eta = 0.45$. It is obtained by taking the ratio of the $Q_i(u+d)$ muons charge signal distribution and the noise width:

$$\left(\frac{S}{N}\right) = \frac{Q^{\mu}_{u+d}}{\sigma^{Ped}}$$

as was used in [13]. The S/N separation is depicted in Figure 9 for cells A5, BC5 and D2 and the corresponding tower where all three cells are included. As the signal is the sum of the individual charge in different PMTs, the noise has been treated in a similar way. From the histograms it is clear that the signal is well separated from the noise, although a small overlap between signal and noise is observed for the A and D cells. In Table10 the used values and the calculated S/N

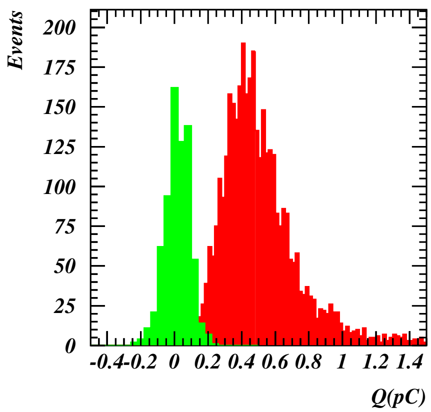

(a) Cell A5

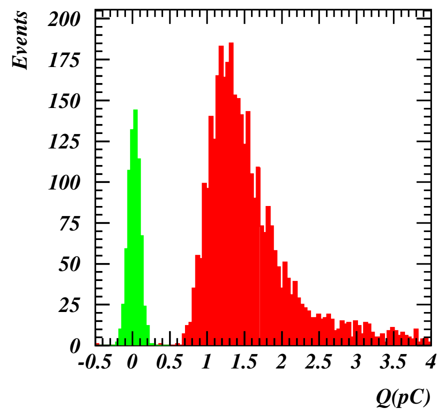

(b) Cell BC5

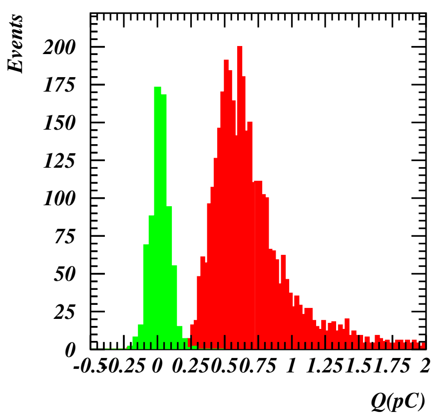

(c) Cell D2

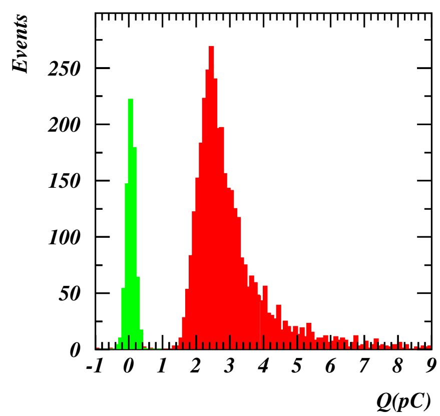

(d) Tower η = 0.45

Figure 9: Signal noise separation for 180 GeV muons crossing a Central Barrel TileCal module for a projective trajectory of η = 0.45 (Flat Filter event reconstruction method)

	PMT # Up/Down	Q^{μ}_{u+d} (pC)	σ^{μ}_{Gauss} (pC)	Q^{Ped}_{u+d} (pC)	σ^{Ped} (pC)	$\left(\frac{S}{N}\right)$
A cell	20/21	0.429	0.018	0.136	0.071	6.04
BC cell	22/23	1.262	0.022	0.242	0.075	16.83
D cell	26/27	0.560	0.019	0.142	0.067	8.36
Tower	ALL 6	2.418	0.06	0.385	0.124	19.5
1996	4 PMTs	2.66	–	–	0.068	39.0

Table 10: Signal to noise ratio, using the Flat Filter energy reconstruction Method, for muons crossing the calorimeter for a projective trajectory of $\eta = 0.45$. Data from July 2002 using Barrel Module JINR 55. The 1996 are results for the prototypes using projective 150 GeV muons [13]. In energy units and since we have 1.2 pC/Gev, 0.136 pC is ~ 113 MeV and so forth.

for the different cases are presented. The $Q^{\mu}_{u+d} \equiv MOP$ for the present calculation. From the calculated values it is observed that BC cells present the largest value, an intermediate value is obtained for D cells and the smallest for the A cells, in agreement with the number of tiles and tile sizes in each sampling. The $\left(\frac{S}{N}\right)$ for the whole tower is approximately 20, which is half of what was measured during 1996 for the prototypes [13]. An important aspect is that σ_{Ped} is 2x larger in the used reconstructed data (Flat Filter), which simply reduces by half the calculated value of $\left(\frac{S}{N}\right)$. Regarding these comparisons with the 1996 results it should be remarked that:

1. The modules had different radial lengths being larger in 1996;
2. The PMT's used in 1996 were different;
3. In 1996 only the two most energetic cells (4 PMTs) were considered but now the tower uses 6 PMTs;
4. The event reconstruction method was different;

4. Conclusions

In this note the number of photoelectrons per unit of deposited energy (GeV), N_{pe}, for TileCal was measured for 6 Central Barrel production modules using high energy muon beams. Sets of runs of 180 GeV muons entering the detector at $\theta = \pm 90^\circ$ ($\eta = \pm\infty$) were used to measure the N_{pe} in each TileCal cell. This resulted, for each module and beam orientation, in 174 measurements:

$$20[ACells] \times 3 + 18[BCells] \times 3 + 16[CCells] \times 3 + 7[DCells] \times 2 \qquad .$$

A difference of ~ 25% was found between the BASF tiles (~ 100 pe/GeV) and PSM tiles (~ 80 pe/GeV), and this is in agreement with the scintillating tiles light yield differences measured using a radioactive source. The value found for the PSM tiles is in very good agreement with the prediction of 82 pe/GeV, a value obtained using nominal parameters of the detector. The N_{pe} results were further compared with the quantum efficiency of the TileCal photomultipliers and there was no evidence of a relation between quantum efficiency and these N_{pe} measurements. The influence of the N_{pe} on fundamental performance characteristics of the detector as the signal to noise ratio and energy resolution was also investigated. It was shown that with the current light yield level the improovement on the statistical term of the energy resolution is of 3.4%. Between the two producers a difference of 0.2% is obtained in the energy resolution statistical term. The signal to noise ratio for muons was measured to be of the order of 20 for the energy reconstructed with the Flat Filter method; but notice that it is well known the lack of precision of this reconstruction method for pedestal measurements giving signals 2x larger than on TileCal prototypes and presently seen on TileCal production modules when using a different event reconstruction method — Fit method. To conclude, (1) the TileCal detector shows a light yield level compatible with the design requirements for resolution and signal to noise separation and (2) the Slice Method has been found to be an efficient method to measure the N_{pe}, in agreement with simple characteristics of the detector as the PMT gain and energy scale for electrons.

5. Acknowledgment

The work described in this document was supported by a grant within the project 'Calorímetria para ATLAS/LHC' POCTI/FNU/49527/2002.

References

[1] TileCal Collaboration 'Tile Calorimeter Technical Design Report' CERN/LHCC 96-42

[2] A. Bernstein et al. 'Beam tests of the ZEUS barrel calorimeter' Nucl. Inst. and Meth. in Phys.,A336:23-52, 1993.

[3] J. Proudfoot, R. Stanek 'An Optical Model for the Prototype Module Performance from Bench Measurements of Components and the Test Module Response to Muons' ATL-TILECAL-95-066 Geneva : CERN, 25 Oct 1995

[4] J. Proudfoot 'Light yield in the extended barrel prototype modules from electrons at 90 degrees' ATL-TILECAL-97-133 Geneva : CERN, 28 Nov 1997

[5] S. Néme cék, T. Davidek, R. Leitner 'Light Yield Measurement of the 1998 Tile Barrel Module0 using muon beams' ATL-TILECAL-99-003 Geneva : CERN,1 Feb 1999

[6] V. Castillo, F. Fassi 'Light yield and uniformity of the TileCal Barrel Module 0 prototype' ATL-TILECAL-2000-001 Geneva : CERN, 13 Jan 2000

[7] Z. Azaltouji et al. 'Response of the ATLAS Tile calorimeter prototype to muons' Nucl. Inst. and Meth. in Phys, A388:64-78, 1997.

[8] S. Tokar 'PMT Excess Factor' TileCal Week/Tools and MC Session, 15 Oct 2001

[9] V. Garde 'Controle et etalonnage par lumiére laser et par faisceaux de muons du calorimétre hadronique a tuiles scintillantes d'ATLAS' Université Blaise Pascal, 2003

[10] T. Davidek, R. Leitner 'Parametrization of the Muon Response in the Tile Calorimeter' ATL-TILECAL-97-114 Geneva : CERN, 10 Apr 1997

[11] http://altair.ihep.su/ konstant/qc/scintillator.html

[12] http://tilecal.in2p3.fr/pmt/accueil/accueil.php

[13] S. Alkhamadaliev et al. 'Results from a new combined test of an electromagnetic liquid argon calorimeter with a hadronic scintillating-tile calorimeter' Nucl. Inst. and Meth. in Phys., A449:461 477, 2000.

A. Light Yield measurements

For each cell type (A, B, C, D) the N_{pe} is the average over the tilerows (3, 3, 3, 2) and cells (20, 18, 16, 7).

A.1. N_{pe} for the 2002 test beam period

JINR	$\theta = -90°$			$\theta = +90°$		
34	# cells	N_{pe}	rms%	# cells	N_{pe}	rms%
A	51	83.6	5.6	54	81.1	8.6
B	45	101.9	10.4	42	95.8	10.3
C	42	100.7	9.7	42	95.2	8.9
D	14	104.5	8.2	14	98.2	9.2

JINR	$\theta = -90°$			$\theta = +90°$		
55	# cells	N_{pe}	rms%	# cells	N_{pe}	rms%
A	48	82.2	6.4	48	82.3	6.9
B	48	100.6	8.9	51	98.7	12.1
C	48	100.3	8.2	48	98.7	8.9
D	14	98.9	5.1	14	99.5	4.9

JINR	$\theta = -90°$			$\theta = +90°$		
01	# cells	N_{pe}	rms%	# cells	N_{pe}	rms%
A	54	77.0	7.7	54	73.2	8.0
B	46	81.3	6.7	48	81.0	8.1
C	45	82.5	8.6	42	82.1	6.4
D	12	74.2	6.3	10	73.3	6.5

Table 11: The number of photoelectrons per unit of deposited energy (GeV) for the TileCal Central Barrel modules used in the 2002 TB. The average per cell type — A,B,C and D — is given. The error — rms — is presented as a percentage for comparison between cell type.

A.2. N_{pe} for the 2003 test beam period

JINR	$\theta = -90°$			$\theta = +90°$		
27	# cells	N_{pe}	rms%	# cells	N_{pe}	rms%
A	56	78.1	14.6	54	68.0	13.3
B	46	80.9	12.3	45	79.6	11.3
C	43	81.7	11.6	38	78.3	11.6
D	14	99.6	7.6	14	97.5	5.3

JINR	$\theta = -90°$			$\theta = +90°$		
63	# cells	N_{pe}	rms%	# cells	N_{pe}	rms%
A	51	79.9	12.4	40	72.3	12.8
B	38	84.8	9.5	43	85.4	10.9
C	35	88.7	9.0	40	85.5	10.4
D	10	97.4	7.3	12	100.5	10.0

JINR	$\theta = -90°$			$\theta = +90°$		
13	# cells	N_{pe}	rms%	# cells	N_{pe}	rms%
A	53	72.5	13.3	49	63.1	14.3
B	50	79.5	13.7	51	80.1	17.3
C	42	79.7	11.6	46	76.5	14.1
D	14	84.7	8.6	14	81.7	6.9

Table 12: The number of photoelectrons per unit of deposited energy (GeV) for the TileCal Central Barrel modules used in the 2003 TB. The average per cell type — A,B,C and D — is given. The error — rms — is presented as a percentage for comparison between cell type.

B. Settings of PAW and differences on the presented data

In some steps the present analysis the use of means and root mean squares (rms) is needed. Altough the PAW analysis package provides these quantities some care in their interpretation is needed since, by default, these are weighted quantities over the binning, e.g., the mean is

$$< x >= \frac{\sum_{i=1}^{nbin} c_i \times n_i}{\sum_{i=1}^{nbin} n_i} = \frac{\sum_{i=1}^{nbin} c_i \times n_i}{N} \tag{5}$$

and not the real mean as given by:

$$< x >= \frac{\sum_{i=1}^{N} x_i}{N} \tag{6}$$

where,

x is the quantity we are measuring;

$nbin$ is the number of bins in the histogram;

c_i is the value of x that corresponds to the mean point of bin **i**;

n_i is the number of entries in bin **i**;

N is the total number of events.

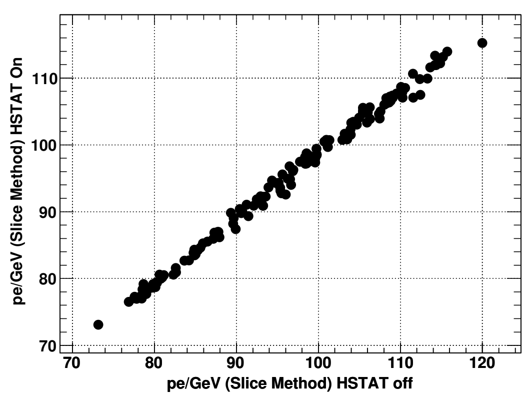

Figure 10: Comparing two PAW settings for the retrieving of statistical information from histograms. A linear fit to the points gives **y** = (0.957 ± 0.007) × **x** + (2.8 ± 0.7).

The real mean (Eq. 6) can be obtained if we set within the PAW session the option 'OPTION HSTAT'. During the analysis described in this note we have used the default settings in PAW and so the undesired mean was used. For future reference the numbers for $\theta = 90°$ were recalculated setting this option ON and a

Tile Row	HSTAT On		HSTAT Off	
	PSM	BASF	PSM	BASF
1-3	78.0± 0.5	—	78.8± 0.5	—
4-6	79.0± 0.7	99.6± 1.0	80.5± 0.8	96.4± 1.0
7-9	80.1± 0.8	99.5± 0.9	81.3± 0.9	97.2± 0.9
10-11	79.2± 1.5	100.4± 1.1	79.8± 1.6	100.3± 1.2

Table 13: The number of photoelectrons per GeV for 90° muons, in Tilecal barrel modules. The mean value and statistical error for each cell type are given separately for PSM and BASF scintillators.

comparison is presented in Figure 10. The plot in Figure 10 and summary table Table 13 show that the differences that result from the comparison of both cases are not important for the definition of the light yield level obtained using high energy muon beams.